

Selective and Accurate Quantification of *N*-Acetylglucosamine in Biotechnological Cell Samples via GC–MS/MS and GC–TOFMS

Teresa Mairinger, Michael Weiner, Stephan Hann, and Christina Troyer*



Cite This: *Anal. Chem.* 2020, 92, 4875–4883



Read Online

ACCESS |



Metrics & More

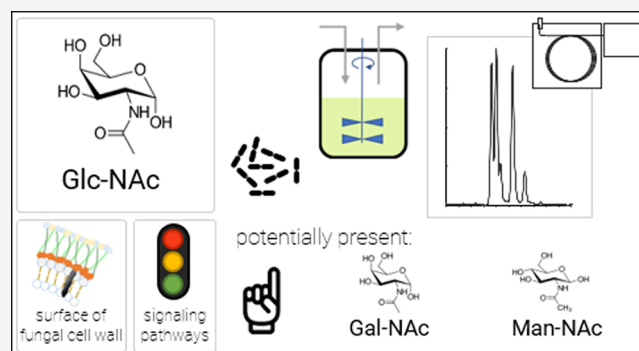


Article Recommendations



Supporting Information

ABSTRACT: *N*-Acetylglucosamine is a key component of bacterial and fungal cell walls and of the extracellular matrix of animal cells. It plays a variety of roles at the cell surface structure and is under discussion to be involved in signaling pathways. The presence of a number of *N*-acetylhexosamine stereoisomers in samples of biological or biotechnological origin demands for dedicated high efficiency separation methods, due to identical exact mass and similar fragmentation patterns of the stereoisomers. Gas chromatography offers high sample capacity, separation efficiency, and precision under repeatability conditions of measurement, which is a necessity for the analysis of low abundant stereoisomers in biological samples. Automated online derivatization facilitates to overcome the main obstacle for the use of gas chromatography in metabolomics, namely, the derivatization of



The separation of naturally occurring isomers with identical exact mass and similar fragmentation patterns is a prerequisite for their accurate quantification and is still a challenging task in metabolomics. Present at low concentrations in complex and concentrated matrices, many isomers (namely, sugars and their derivatives) demand for highly efficient separation methods tolerating high sample loads, as well as selective and sensitive detection methods.

Three *N*-acetylhexosamines occur naturally, with *N*-acetylglucosamine (GlcNAc) being increasingly in the focus of interest of biological studies. This metabolite is under discussion to be involved in cell signaling. Additionally, it is a key component of bacterial and fungal cell walls as well as the extracellular matrix of animal cells and hence plays a variety of roles at the cell surface structure.^{1–3} Besides GlcNAc, *N*-acetylmannosamine (ManNAc) and *N*-acetylgalactosamine (GalNAc) can be present in biological samples. ManNAc plays an essential role in the synthesis of sialic acids like *N*-acetylneuraminic acid.⁴ GalNAc is described as cell-wall monomer⁵ and connects carbohydrate chains in mammalian mucins.⁶ Hence, the development of analytical methods for the

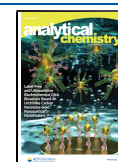
analysis of GlcNAc must take these two potential interferents into account.

Generally, the analysis of monosaccharide derivatives is achievable using gas (GC) and liquid chromatography (LC) based separation. While several separation approaches are described in the literature for hexosamine stereoisomers,^{7–11} to our knowledge, no analytical method separating all three biologically relevant *N*-acetylated hexosamines is available for absolute quantification. To increase the (steric) selectivity and realize separation, derivatization often comes into play.¹² This holds true not only for GC based approaches, where derivatization is considered as standard sample preparation when dealing with polar analytes, but also for LC based methods. Besides separation, the development of quantitative

Received: October 8, 2019

Accepted: February 25, 2020

Published: February 25, 2020



techniques for the *N*-acetylglucosamine determination poses further challenges. The derivatization of complex molecules with a high number of functional groups is neither quantitative nor matrix independent.^{13,14} Hence, it is of utmost importance to control derivatization conditions. Besides, the matrix dependent derivatization yield especially demands the application of suitable correction strategies like the gold standard, i.e., internal standardization with heavy stable isotope labeled analogues of the analyte of interest representing.

For gas chromatography (GC), two-step derivatization methods based on alkoxylation and trimethylsilylation have long been used for the analysis of sugars and their derivatives.^{15,16,11,17} Alkoxylation converts the ketone or aldehyde carbonyl group into alkoxyamino groups while shifting the equilibrium from the cyclic to the open chain structure, which results in simpler chromatograms due to the reduction of the number of isoforms present in the measurement solution.¹⁵ Nevertheless, the number of naturally occurring isomers is multiplied by trimethylsilylation due to partial derivatization of certain functional groups like amino groups.

For selective analysis of carbohydrate isomers, it is of utmost importance to carefully select and control derivatization conditions in order to ensure chromatographic separation of the derivatives of interest. Directing derivatization toward a certain derivative can be realized by optimizing conditions in terms of temperature and incubation time. The best control of derivatization can be achieved using automated just-in-time derivatization enabling instant gas chromatography–mass spectrometry (GC–MS) analysis of the sample.

In case of *N*-acetylhexosamines, the observation of different derivatives exhibiting four and five trimethylsilyl (TMS) groups can be explained by the lower reactivity of the secondary amino group.^{18,19} For the present approach, derivatization was steered toward the 4TMS derivatives, which showed a significantly higher intensity even using non-optimized derivatization conditions. Hence, GC separation was optimized for the 4TMS derivatives of different naturally occurring *N*-acetylhexosamines. Apart from efficient chromatographic separation, the compensation of systematic errors related to matrix effects is also a necessity for accurate quantification. Since matrix effects are compound dependent, this compensation needs to be based on chemically identical stable isotope labeled internal standards. Highly complex and concentrated matrices additionally demand for selective MS detection, using either high-resolution accurate mass MS instrumentation or tandem MS devices with, e.g., collision induced dissociation.

By applying this concept, *N*-acetylglucosamine could be quantified in various sample types of *Penicillium chrysogenum* cultivations, i.e., intracellular cell extracts, cell culture supernatants, and the corresponding quenching and washing solutions, which proved this optimized method as highly rugged for the analysis of different matrices.

■ EXPERIMENTAL SECTION

Chemicals. *N*-Acetylglucosamine (GlcNAc) ($\geq 98\%$), *N*-acetylgalactosamine (GalNAc) ($\geq 98\%$), and *N*-acetylmannosamine (ManNAc) ($\geq 98\%$) were purchased at Sigma-Aldrich (Sigma-Aldrich, Vienna, Austria). ¹³C₆-*N*-Acetylglucosamine was purchased at Omicron (Omicron Biochemicals Inc., South Bend, Indiana). *O*-Ethylhydroxylamine hydrochloride (EtOX, 97%) and *O*-methylhydroxylamine hydrochloride (MOX, >

98%) were obtained from Sigma-Aldrich. *N*-methyl-*N*-(trimethylsilyl) trifluoroacetamide (MSTFA) and 1% trimethylchlorosilane (TMCS) were purchased from Macherey-Nagel (Macherey-Nagel GmbH, Dueren, Germany). Pyridine water free (99.8%) and pyridine ($\geq 99.9\%$) for syringe washing were purchased at Sigma-Aldrich.

Stock solutions of all compounds and the working standards were prepared daily by dissolving the standard in Chromasolv LC–MS Ultra water (Honeywell Riedel-de Haën, Fisher Scientific, Vienna, Austria) in amber vials.

Biotechnological Synthesis of U¹³C Internal Standard (IS). U¹³C labeled cell extract of *Pichia*, which had been produced as described in detail by Neubauer et al.,²⁰ was purchased from ISOTopic Solutions (ISOTopic Solutions, Vienna, Austria). Uniformly ¹³C labeled *Penicillium* extract and supernatant were prepared by fed-batch cultivation of *Penicillium chrysogenum* on fully ¹³C labeled glucose, as described by Meinert.²¹ The fermentation broth was quenched and filtered. The washed cells were extracted using cold extraction techniques. For methodical details of biomass inactivation and extraction, see the [Sampling, Quenching, and Extraction of Biological Samples](#) section.

For the preparation of the internal standard, the U¹³C cell extracts and supernatant were mixed in order to provide a broad range of intra- and extracellular metabolites for the use in multicomponent methods.

Sampling, Quenching, and Extraction of Biological Samples. The sampling of cell broth from a *Penicillium chrysogenum* cultivation, as well as sample preparation, was performed as described previously.²² Within this procedure, an automated sampling device was used for the withdrawing of culture broth and for sampling. In combination with cold methanol quenching (60% methanol, $-40\text{ }^{\circ}\text{C}$, quenching ratio 1:3), this device was used for the rapid inactivation of cell metabolism. The samples were vacuum-filtered through a nylon filter. Subsequently, the biomass was washed using the initially applied quenching solution. Afterward, the biomass sample was transferred into a cold methanol–buffer (1:1 (v/v) mixture of methanol and TE buffer (10 mM TRIS, 1 mM EDTA, pH 7.0), $-40\text{ }^{\circ}\text{C}$) and stored in liquid nitrogen until extraction. Biomass extraction was performed using chloroform (extraction ratio 1:1). After 24 h, an end-over-end rotation ($-20\text{ }^{\circ}\text{C}$), a centrifugation step (10 000g, 10 min, $-11\text{ }^{\circ}\text{C}$), followed by collection of the upper phase and subsequent filtration (0.2 μm) were performed.

Automated Derivatization. The two-step derivatization of samples and standards with (1) ethylhydroxylamine or methylhydroxylamine hydrochloride and (2) MSTFA with 1% TMCS was performed automatically on a Gerstel MPS2 dual rail sample preparation robot (Gerstel GmbH, Muehlheim, Germany). The robot was equipped with two parallel rails, each carrying a robotic tower capable of performing independent liquid handling steps. One tower was equipped with a 10 μL syringe for sample injection; the second tower was equipped with a 100 μL syringe for the addition of the reagents. Both towers were also in use for transportation of the samples. Each rail was equipped with a heated agitator for derivatization. Underivatized dried samples were stored at $6\text{ }^{\circ}\text{C}$ in a cooled stack until the onset of just-in-time derivatization. Reagents were stored at $6\text{ }^{\circ}\text{C}$ in a Peltier cooled tray. Sample preparation as well as the injection were controlled by the Maestro software package 1.4.30.6. (Gerstel), which was linked

with the MassHunter Acquisition software B07.06 (Agilent Technologies Inc.).

For derivatization and analysis, aliquots of 60 μL of standards, 50 μL of extracts, 80 μL of washing and quenching solutions, and 120 μL of the cultivation supernatant were used. The ratio of internal standard volume/sample volume was 0.2 for extracts, 0.15 for washing and quenching solutions, and 0.1 for supernatants.

20 μL of *O*-ethylhydroxylamine hydrochloride in pyridine ($c(\text{EtOX}) = 20 \text{ mg mL}^{-1}$) was added to the spiked samples and standards prior to drying in a vacuum centrifuge, in order to prevent the degradation of keto carbonyl group containing compounds.²³ The samples were evaporated to complete dryness at pressures of <1 mbar to ensure efficient and quick drying at low temperatures. Dried samples were immediately crimped with magnetic caps to enable transportation on the robot and were placed in the drawer cooled stack (6 °C) of the MPS 2 autosampler until derivatization. If dried samples were not analyzed within 24 h, they were redried before analysis. In the first derivatization step, the samples were dissolved in 18 μL of water-free pyridine containing 19 mg mL^{-1} EtOx. The samples were incubated (25 °C, 120 min) under agitation (250 rpm) to convert ketone and aldehyde carbonyl groups into ethylhydroxylamino groups. Subsequently, 42 μL of MSTFA with 1% TMCS were added and the samples were heated and agitated (250 rpm) at 40 °C for 50 min to replace acidic protons by trimethylsilyl groups. Syringes were washed with pyridine before and after each liquid dosage. After a cool down to room temperature for 1.5 min in an open tray of the MPS2, samples were cooled in the cooled stack at 6 °C for 5 min and were then injected for GC–MS analysis. After injection, samples were placed back into the cooled tray at 6 °C. Derivatization was controlled by Maestro software package (Gerstel). Sequences were scheduled in a way that samples were derivatized during the GC runs of the preceding samples, hence enabling injection of the derivatized samples immediately after sample preparation was finished.

GC–MS/MS and GC–TOFMS Analysis. GC separation was carried out on Agilent 7890B gas chromatographs coupled either with an Agilent Technologies 7200B Q-TOF (GC–TOFMS) mass spectrometer or with an Agilent Technologies 7010B Triple Quadrupole (GC–MS/MS) mass spectrometer (Agilent Technologies Inc.). Both GC–MS systems were equipped with (1) a nonpolar deactivated precolumn (3 m \times 0.25 μm i.d., Phenomenex), which was connected to the analytical column via a backflush unit (purged ultimate union), and (2) a nonpolar deactivated postcolumn (3 m \times 0.18 μm i.d., Phenomenex), which was connected with the analytical column via a second ultimate union T-piece serving as a restrictor column to the MS. The following analytical columns were tested: ZORBAX DB-5MS + 10 m Duragard capillary column (5% phenyl–95% dimethylpolysiloxane, 30 m \times 250 μm \times 0.25 μm) from Agilent Technologies Inc., and Optima 5 MS Accent (5% phenyl–95% dimethylpolysiloxane, 60 m \times 250 μm \times 0.25 μm) and Optima 1 MS Accent (100% dimethylpolysiloxane, 30 m \times 250 μm \times 0.25 μm), both from Macherey Nagel.

The GC–QTOFMS instrument was equipped with an Agilent split/splitless injector, whereas the GC–MS/MS was equipped with an Agilent Multi Mode Inlet. Agilent Ultra Inert splitless liners with a single taper were used. Sample aliquots of 1 μL were injected in the splitless mode (220 °C, splitless time 2 min, septum purge flow 3 mL min^{-1}). The following GC–

temperature program was used: 70 °C (hold for 1 min), 30 °C min^{-1} to 240 °C, 2 °C min^{-1} to 260 °C, with 30 °C min^{-1} to 310 °C (hold for 3 min). The transfer line to the MS was kept at 280 °C. Helium 5.0 was used as carrier gas with a constant flow of 1.1 mL min^{-1} for the precolumn, 1.2 mL min^{-1} for the analytical column, and 1.4 mL min^{-1} for the post column. The electron ionization (EI) source of the instruments was operated with an electron energy of 70 eV and an emission current of 35 μA for the QTOF and 100 μA for the MS/MS at a temperature of 230 °C. For both instruments, the quadrupole was set at 150 °C. For chemical ionization (CI), an emission current of 10 μA was used, the ion source was operated at 150 °C, and a reagent gas flow of 20% CH_4 (corresponding to 1 mL min^{-1}) was employed.²⁴ The QTOF was operated in TOF-mode with a scan speed of 3.33 Hz and in 2 GHz Extended Dynamic Range mode. The mass accuracy was <2 ppm for the calibration ions and resolution at approximately 8000 R_{FWHM} at m/z 501.9706. Mass spectra were acquired in profile mode and were converted postacquisition to centroid. The GC–MS/MS system was operated with 3.5 Hz, and the resolution was set to widest (corresponding to a mass isolation window of 2.5 m/z) for both mass selective quadrupoles. For data evaluation, MassHunter Quantitative analysis B.08.00 (Agilent Technologies Inc.) was used.

RESULTS AND DISCUSSION

Derivatization. Two-step derivatization enabling the conversion of a wide range of polar functional groups was applied to guarantee GC amenability. In the first step, alkoxylation converts the aldehyde carbonyl group of the *N*-acetylhexosamines into an alkoxyamino group, thereby opening the ring structure and forming a *cis* and a *trans* isomer. Amide carbonyl groups are not converted.^{13,25} In the second step, trimethylsilylation replaces the active hydrogen atoms of the hydroxyl groups and, to a smaller extent, also the less reactive hydrogen atom of the secondary amino group by trimethylsilyl groups. The formation of several derivatives for a single metabolite is a common observation for metabolites exhibiting amino groups or high numbers of other acidic hydrogen atoms, since alkoxylation and trimethylsilylation are known to be incomplete.^{13,18} Besides, it was also reported that, compared to Si–O bonds, Si–N bonds are more labile, and hence, fully labeled TMS derivatives were not suitable for quantification.¹⁸ As a matter of fact, derivatization efficiency was roughly estimated to be in the range 25%–110% for amino acids, 60%–90% for organic acids, and 80%–115% for monosaccharides and sugar alcohols, which are less complex molecules exhibiting a lower number of functional groups than *N*-acetylhexosamines.¹³ Since both the 4TMS and the 5TMS derivatives can be detected for *N*-acetylhexosamines,¹⁹ the use of isotope labeled internal standards (see further discussion in the **Internal Standardization** section) or mathematical correction strategies for quantitation²⁶ are required.

The fact that derivatization is highly matrix dependent,²⁷ whereby the matrix can catalyze or suppress derivatization, strongly affects derivatization efficiency as well as the ratio of the 4TMS and 5TMS derivatives. In contrast to Gullberg et al.,¹⁹ derivatization and injection parameters were optimized in order to steer the derivatization toward the formation of the 4TMS derivative. This derivative showed higher intensity in comparison to the 5TMS derivative, using incubation times of less than 3 h. This is in accordance to findings in the literature.¹⁸ The inlet temperature was set to as low as 200 °C

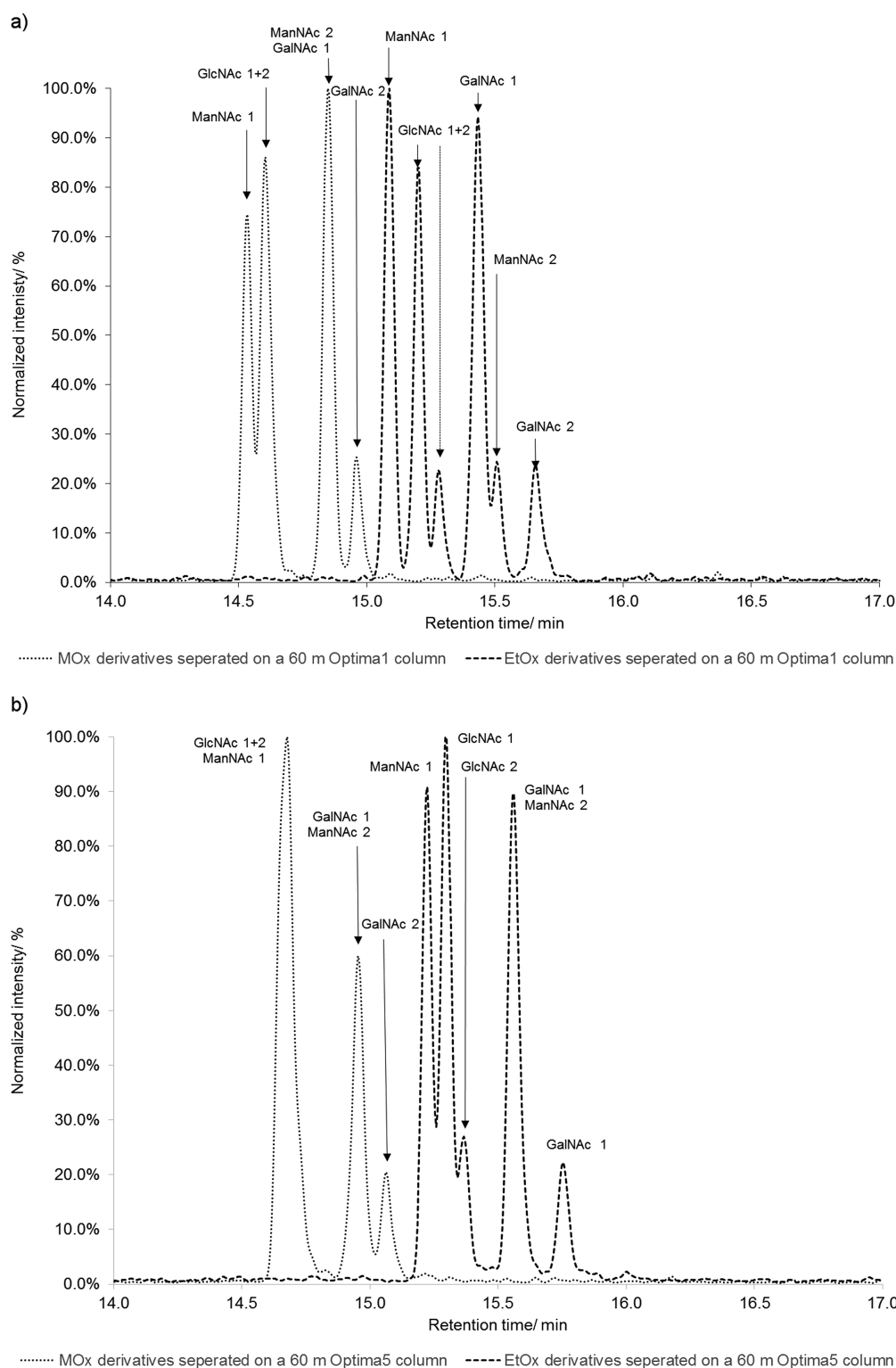


Figure 1. Extracted ion chromatograms (GC-Cl-TOF) of the three biologically relevant N-acetylated hexamines, i.e., N-acetylglucosamine (GlcNAc), N-acetylgalactosamine (GalNAc), and N-acetylmannosamine (ManNAc), using two different oximation reagents, namely, MOX and ETOX (dotted and dashed lines, respectively). For this purpose, the $[M - \text{CH}_3]^+$ of the respective *cis* and *trans* 4TMS derivative was extracted. (a) Separation using a 60 m Optima 1 MS column is depicted. (b) Separation using a 60 m Optima 5 MS is shown.

to prevent the formation of the 5TMS derivative in the inlet, which explains the decrease of signal intensity with temperature, as shown in Figure S1 in the Supporting Information for inlet temperatures of 200–260 °C.

It is worth mentioning that optimization of derivatization conditions is always multifactorial, and often, rather broad optima are observed. For rough optimization, the following settings were tested: 30, 40, 55, and 70 °C and derivatization times of 60, 120, and 180 min for ethoximation and

temperature settings of 25, 40, 55, and 70 °C and derivatization times of 50 and 90 min for silylation. The results on the optimization of ethoximation and silylation are shown in the Supporting Information, Figures S2 and S3, using GC–CI–MS/MS in SIM mode, m/z 537.3, representing the $[M - CH_3]^+$ of the 4TMS derivative. For ethoximation, low temperatures proved to be more advantageous in terms of signal intensity. Regarding the optimum temperature value for the ethoximation step, a rather broad range was observed, with no significant difference between 30 and 40 °C. Hence, to increase universal applicability, 25 °C (to simulate room temperature) for 120 min were chosen as the final derivatization conditions.

For silylation, 50 min incubation time at a temperature of 50 °C was chosen. No additional benefit was found for longer derivatization, i.e., 90 min compared to 50 min. As for temperature, the most commonly applied settings, namely, in the range 40–50 °C,^{23,13,10} proved to be valid also for this compound class.

In summary, alkoximation was performed at 25 °C for 2 h and trimethylsilylation at 50 °C for 50 min. With regard to the matrix dependence of the derivatization, optimum parameters for maximum derivatization efficiency as well as sole formation of the 4TMS derivative may vary depending on the sample type. Hence, it has to be pointed out that the optimized derivatization parameters have to be considered as an estimation for real samples. As a consequence, the aim was to ensure sufficient intensity of the 4TMS derivative.

Chemical ionization confirmed the presence of the 4TMS derivative in the GC–MS chromatogram, whereas the 5TMS derivative could be detected neither in standards nor in *P. chrysogenum* samples using the optimized derivatization and injection conditions.

The aforementioned matrix effect demands for correction of the inherent systematic error in derivatization efficiency for accurate quantitative analysis. Especially in biotechnological samples, matrix composition can change vastly between sample types (e.g., cell extracts, supernatants, quenching solutions, and washing solutions) and even between samples of the same type but that are taken at different time points in fed-batch or batch experiments.

Interconversion of the three *N*-acetylhexosamines was tested by the analysis of single standards. These experiments were carried out with pure standards, as well as standards spiked with the biologically derived ¹³C labeled internal standard in order to check for matrix influences. Using the optimized analytical method, no interconversion was observed.

In order to minimize manual work and improve precision of derivatization, automated just-in-time online derivatization was established using a derivatization robot (Gerstel). In contrast to the offline derivatization of sample batches, the derivatization time is constant for all samples of a batch using online derivatization and just-in-time injection. This is of special importance for the derivatization of the *N*-acetylhexosamines, which are derivatized at low temperatures close to room temperature, which means that the derivatization reaction might continue even on the cooled autosampler when offline derivatization is used.

Chromatographic Separation. Chromatographic selectivity and efficiency were optimized with respect to the separation of the three naturally occurring *N*-acetylhexosamine isomers, namely, *N*-acetylglucosamine, *N*-acetylgalactosamine, and *N*-acetylmannosamine. Chromatographic separation of

these three isomers is essential due to the highly similar mass spectrometric properties of their derivatives using electron ionization (see the Supporting Information, Figure S4).

For polar metabolites showing a high number of diverse functional groups, the most widely used analytical method is oximation with methylhydroxylamine, subsequent trimethylsilylation, and GC separation on 5% phenyl 95% methyl silicone columns (30 m × 0.25 mm i.d. × 0.25 μm film thickness).¹⁰ However, by applying this method, the methoximated derivatives of the three hexosamines could not be separated (see the Supporting Information, Figure S5). Hence, different stationary phase chemistries were tested and, although the use of long GC columns should be avoided, high column bleed when using longer columns and long separation times are no longer an issue in modern GC with low bleed MS columns and temperature programming. Besides the increase in resolution by the square root of the column length, i.e., factor 1.4 here, can be critical, especially when dealing with stereoisomers.

Since trimethylsilylated compounds are nonpolar, 100% dimethylpolysiloxane and 5% phenyl 95% dimethylpolysiloxane as stationary phases were tested. Separation was optimized for both methoximated and ethoximated derivatives using low bleed 60 m columns (i.d. 0.25 mm, film thickness 0.25 μm). Columns with smaller inner diameter or thinner films also capable of improving separation efficiency were not tested, since the highly concentrated and complex matrix of samples from biotechnological batch and fed-batch cultivations would overload columns of lower sample capacity. The optimization of the temperature program aimed at high resolution and short run times in order to minimize the longitudinal diffusion of the employed 60 m columns. To benefit from solvent focusing, the ramp started at 70 °C and increased rapidly to 240 °C to minimize the longitudinal diffusion. Since the use of temperature ramps <2 °C min⁻¹, and an earlier onset of this slow temperature gradient, did not lead to a more efficient separation of the isomers, the temperature gradient continued as following: 240 °C, 2 °C min⁻¹ to 260 °C. Finally, the oven temperature was increased to 310 °C at a rate of 30 °C min⁻¹ and held for 3 min.

For all the combinations tested, the best separation was achieved for ethoximated derivatives on the 100% dimethylpolysiloxane column, as can be seen in Figure 1 (baseline separation of ManNAc and GlcNAc within less than 16 min).

Since the first ManNAc derivative elutes prior to the GlcNAc derivatives on both column types, quantitative GlcNAc analysis might be hampered by high ManNAc concentrations resulting in deteriorated validation parameters like higher LOQ. However, in contrast to GalNAc, ManNAc could not be detected in *Penicillium chrysogenum* samples during prior testing of samples and methods. This result is in accordance with the fact that both main components of the fungal cell wall (chitin and β-glucans)², which are built of a polysaccharide structure of *N*-acetylglucosamine (chitin) and, respectively, α1–4 linked galactose and α1–4 linked *N*-acetylgalactosamine (β-glucans),²⁸ are not based on *N*-acetylmannosamine.

As a consequence of the preliminary testing, which showed the absence of ManNAc in the *P. chrysogenum* samples, both columns types were considered equally suitable for the analysis of GlcNAc in *P. chrysogenum*. Due to the fact that 5% phenyl 95% methylsiloxane columns are in wide use in the area of GC based metabolomics, the present work was carried out using

Table 1. Optimized Parameters for the Quantitative Analysis of *N*-acetylglucosamine by Triple Quadrupole Mass Spectrometry^a

analyte	retention time (min)	quantifier			qualifiers		
		precursor ion (<i>m/z</i>)	product ion (<i>m/z</i>)	CE (V)	precursor ion (<i>m/z</i>)	product ion (<i>m/z</i>)	CE (V)
GlcNAc	14.08	347.2	288.1	5	347.2	101.0	5
					537.3	147.1	30
U ¹³ C ₆ GlcNAc	14.08	353.2	292.2	5	353.2	292.2	5
					545.3	147.1	30

^aPrecursor and product ion *m/z* ratios are listed together with the employed collision energy and retention time.

5% phenyl 95% dimethylpolysiloxane columns (60 m × 0.25 mm × 0.25 μm).

Mass Spectral Detection Using TOFMS and MS/MS. In fact, compared to mass analyzers such as triple quadrupoles, accurate mass time-of-flight instruments do have a limited linear dynamic range and detector saturation effects for some compounds' ions occur quite regularly when dealing with biological samples. However, since in TOFMS a full mass spectrum per chromatographic point is acquired, it thereby opens the possibility of increasing the method's linear dynamic range and evading these saturation effects. This can be achieved either by choosing a different, less sensitive EI fragment or by evaluating—instead of the monoisotopic mass—a heavier isotopologue of the respective ion. It is noteworthy that selecting a different EI fragment can be challenging, since it still needs to meet certain criteria, such as selectivity and spacing between the monoisotopic mass and its fully ¹³C labeled analogue, i.e., the internal standard *m/z*. In GC based analysis, the introduction of silicon during the derivatization process leads to a more pronounced isotope pattern compared to that of the native molecule due to its rather highly abundant heavy stable isotopes ²⁹Si and ³⁰Si. This facilitates the practical use of an isotopologue instead of the monoisotopic mass for data evaluation. Considering the [M - CH₃]^{•+} of the 4TMS derivative (537.2662 *m/z*, C₂₁H₄₉N₂O₆Si₄), the use of the M + 1 or M + 2 decreases the response of the signal roughly by a factor of 2 or 3, respectively. In most cases, this is sufficient to extend the linear dynamic range of a TOF method. In the case of GlcNAc analysis with the present setup, the linear range is limited to concentrations up to 10 μmol L⁻¹ using the monoisotopic mass 537.2662 for data evaluation (see Figure S7). The choice of less sensitive isotopologues for data analysis significantly extends the linear range, as is shown in Figure S7 in the Supporting Information. When the isotopologue M + 3 in comparison to the monoisotopic mass 537.2662 is evaluated, the calibration is linear up to 200 μmol L⁻¹. This gain in linear range is accompanied by a loss of sensitivity, which is reflected by higher LOQs (LOQ is increased by roughly a factor of 30) for that data evaluation method. Nevertheless, exploiting the full capacities of TOFMS by retrospective choice of more than one isotopologue for data analysis, the concentration range, which can be covered by TOFMS, is comparable to MS/MS analysis (see the Figures of Merit section). To avoid saturation of the fully ¹³C labeled internal standard mass, the same concept was applied to the internal standard evaluation. For the internal standard, an isotopologue M + 3 in comparison to the mass of the fully ¹³C labeled monoisotopic mass (545.2931) was chosen.

In summary, for TOFMS analysis, the following exact masses were chosen as quantifier ions: *m/z* 537.2662 (low concentrations in samples), 538.2676 (high concentrations in

samples), and the fully ¹³C labeled isotopologue *m/z* 548.3007 as the internal standard ion. The qualifier ions were: 347.1817 (low concentrations), 348.1835 (high concentrations in samples), and the fully ¹³C labeled isotopologue *m/z* 354.2042 as the internal standard ion.

Another aspect to be considered when using accurate mass instrumentation is the extraction window. The mass accuracy obtained on the TOFMS is in the low ppm range (<2 ppm for calibrant ions); however, to guarantee a reasonable signal intensity, the extraction window should be set to at least ±25 ppm. Different extraction windows, namely, 25, 50, 100, 150, and 200 ppm, were checked in terms of selectivity and sensitivity. For all the fragments tested (see Table S1), narrower mass extraction windows did not increase selectivity and therefore a window of 150 ppm (±75 ppm) was chosen to maximize signal-to-noise ratio. It is noteworthy that high resolution is a necessity to suffice selectivity requirements for *m/z* 537.2662 as it is interfered by *m/z* 536.9705.

MS/MS detection was optimized for collision energies ranging from 0 to 40 eV for the following precursor ions: 537.2662 (M-15), 347.1817, and 319.1576 (chemical structures are listed in Table S1). Transitions to unspecific product ions like *m/z* 73 ((CH₃)₃Si⁺) and *m/z* 147 ((CH₃)₃SiOSi(CH₃)₂⁺), which contain no backbone carbon atoms, were avoided if possible. The use of the dominant fragment with the mass-to-charge ratio of 319.1576 shows high sensitivity both in TOFMS and as precursor ion in MS/MS. Nevertheless, as this fragment is a common fragment for sugar derivatives, it can be used neither in TOFMS nor in MS/MS for the analysis of cell samples due to lack of selectivity.

For MS/MS, the qualifier and quantifier transitions were chosen based on selectivity and sensitivity in *Penicillium chrysogenum* samples (extracts, quenching and washing solutions, whole broth supernatant) and are summarized in Table 1. The transitions 347.2 → 288.1 and 347.2 → 101.0 show similar signal-to-noise ratios, as the most sensitive transitions using 319.2 as precursor ion but in contrast to the latter, also high selectivity for the *N*-acetylhexosamines. Moreover, these transitions favor GlcNAc analysis in terms of sensitivity, showing reduced sensitivity for the other *N*-acetylamine isomers (roughly a factor of 6 for ManNAc and a factor of 3 for GalNAc), as depicted in the Supporting Information Figure S6. Transitions from 537.3 are equally selective but generally less sensitive. Hence, for this precursor, the most sensitive transition to an unspecific ion (*m/z* = 147) was chosen and was used as the qualifier.

Exact monoisotopic masses, chemical formulas, and chemical structures of the fragments used for the quantification of *N*-acetylated hexosamines via GC-TOFMS and GC-MS/MS are listed in Table S1 in the Supporting Information.

Internal Standardization. Internal standardization with a chemically identical, isotopically labeled internal standard is a

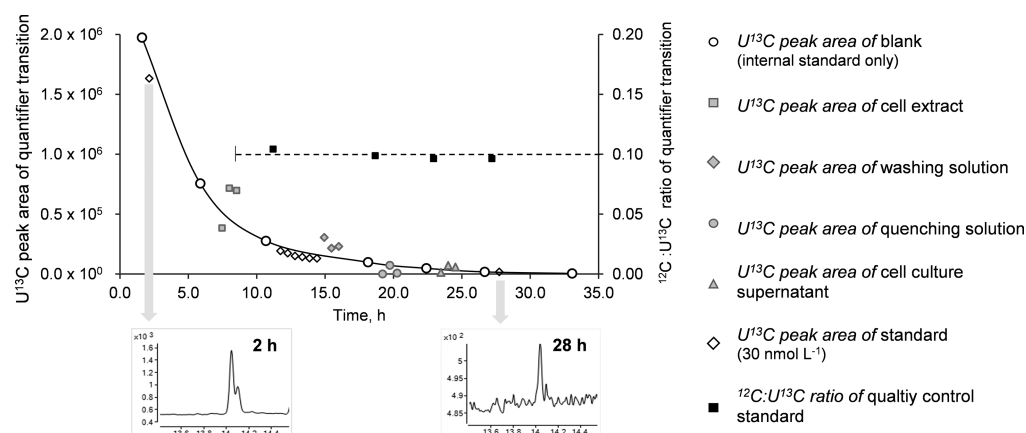


Figure 2. Drift of internal standard signal over the course of a 35 h GC–MS/MS measurement sequence (corresponding to 65 injections). “O” represents the signals of $U^{13}C$ GlcNAc (quantifier transition) in blank samples containing the internal standard over the whole sequence, whereas “□”, “◆”, “●”, and “Δ” represent the internal standard peak areas of $U^{13}C$ GlcNAc in a *Penicillium chrysogenum* cell extract, in the washing solution, the quenching solution, and the cell culture supernatant, respectively. “◇” represents the internal standard signals of a 30 nmol L^{-1} standard, measured at different time points within the sequence. To illustrate the decrease in signal-to-noise of the transition (m/z 347.2–288.1) used as quantifier, an extracted ion chromatogram is shown after 2 and 28 h (data not smoothed), respectively. “■” shows the $^{12}C/^{13}C$ ratio of a quality control standard analyzed repetitively during the sequence.

Table 2. Figures of Merit for GC–MS/MS and GC–TOFMS

	GC–MS/MS	GC–TOFMS		
		m/z 537.2662	m/z 538.2676	m/z 540.2671
LOQ ^a ($\mu\text{mol L}^{-1}$)	0.01	0.04	0.06	1
sensitivity (ratio peak area analyte/ISTD per $\mu\text{mol L}^{-1}$)	0.05	0.84	0.37	0.06
linear range ^b ($\mu\text{mol L}^{-1}$)	0.03–200	0.04–10	0.06–100	1–200
correlation coefficient ^b	0.9993 ($n = 9$)	0.9995 ($n = 6$)	0.9998 ($n = 8$)	0.9998 ($n = 5$)
repeatability QC samples ($c = 2.5 \mu\text{mol L}^{-1}$)	4% ($n = 4, 16 \text{ h}$)	9% ($n = 7, 22 \text{ h}$)	9% ($n = 7, 22 \text{ h}$)	5% ($n = 7, 22 \text{ h}$)
repeatability samples (extracts)	1% ($n = 6, 25 \text{ h}$)	4% ($n = 5, 17 \text{ h}$)	4% ($n = 5, 17 \text{ h}$)	12% ($n = 5, 17 \text{ h}$)

^aCalculated according to Eurachem,²⁴ $n = 8$, $c = 0.05 \mu\text{mol L}^{-1}$ for GC–MS/MS and $c = 0.1 \mu\text{mol L}^{-1}$ for TOFMS ^bCorresponding calibration graphs are depicted in Figure S7 for GC–TOFMS and Figure S8 for GC–MS/MS

prerequisite for GlcNAc quantitation.^{29,20} Internal standardization with heavy stable isotope labeled isotopologues compensates for systematic errors stemming from instrument performance, matrix dependent fluctuations of derivatization efficiency, and, when added early in the sampling process, also certain sample alterations (e.g., decomposition reactions) attributable to extraction, shipment, sample storage, or freezing/thawing.

Hence, absolute quantitation is based on internal standardization with uniformly ^{13}C labeled GlcNAc, which is, among many other metabolites, present in the biologically derived multicomponent internal standard (see the Experimental Section). This standard is routinely added to the biotechnological samples in the course of sampling, especially when multiple metabolites are in scope of analysis.^{29,20} Alternatively, fully ^{13}C labeled GlcNAc is commercially available. However, the use of a pure commercial standard does not provide matrix matching for calibration standards and samples, as is the case with the biologically derived internal standard.

Due to the highly complex matrices of the samples and spiked standards, which are characterized by high contents of organic matter, inlet and ion source performance deteriorate rapidly throughout a sequence. Figure 2 shows the internal standard peak areas ($c^{13}C$ GlcNAc) = $22 \mu\text{mol L}^{-1}$) for samples and calibration standards in a 35 h measurement sequence for the quantitation of GlcNAc in *Penicillium*

chrysogenum samples with GC–MS/MS. The signal of ^{13}C GlcNAc in the internal standard of the blank sample (IS only, depicted as white circles in Figure 2) decreases exponentially over time leading to a continuous decrease of signal-to-noise ratio (see the extracted ion chromatograms for a calibration standard of 30 nmol L^{-1} (MS/MS transition m/z 347.2–288.1) measured at the beginning (after 2 h) of the sequence and after 52 injections (corresponding to 28 h)). It is noteworthy that this drift of absolute intensity does not influence quantification as it is based on signal ratios of chemically identical analyte and internal standard ions. Indeed, the method showed excellent precision under repeatability conditions of measurement. Also, it is worth mentioning that sequences with run times over 36 h are not recommended, since samples would require being redried to guarantee high derivatization efficiency.

Moreover, derivatization efficiency is highly matrix dependent. This is reflected by the internal standard signal measured in calibration standards (30 nmol L^{-1}) as well as the biotechnological samples. It can be clearly seen that $U^{13}C$ peak areas of extracts, supernatants, and washing and quenching solutions taken at different time points of the cultivation show a high variation, indicating the matrix-dependence of derivatization efficiency and hence the need of a suitable internal standardization strategy.

Figures of Merit. Biological samples are characterized by a vast concentration range of diverse metabolites. As a

consequence, some analytes will be present in a high concentration, whereas others are just above LOQ. In GC based separation of small polar metabolites, where derivatization becomes a prerequisite, the sample volume to be dried down prior the derivatization is one parameter to adjust according to the set of analytes. High sample volumes limit the linear range but enable low LOQs if derivatization is not compromised by high matrix load. Hence, sample volume needs to be adapted to sample type, more specifically, GlcNAc concentration and matrix composition. The final sample volumes used ranged from 50 to 120 μL (see the [Experimental Section](#)).

Figures of merit of quantitative GlcNAc analysis based on internal standardization and external calibration were calculated for both GC-MS/MS and GC-TOFMS in measurement sequences of 69 and 53 injection, respectively (figures of merit in [Table 2](#)). Both instruments show high sensitivity and an LOQ of 10 nmol L^{-1} for the MS/MS and 40 nmol L^{-1} for the TOFMS (calculated according to Eurachem³⁰). Excellent selectivity, which is a necessity for biotechnological samples, is achieved using selective transitions for the MS/MS and high resolution at the TOFMS (a minimum resolution of approximately 3500 is needed due to the aforementioned mass spectral interference). Linearity is restricted on the TOFMS in comparison to MS/MS, using the monoisotopic mass of the selective fragment $[\text{M} - \text{CH}_3]^+$ (537.2662). However, due to the possibility of using isotopologues of the respective fragment, the method's linear dynamic range can be extended at the expense of sensitivity and LOQ (see the [Mass Spectral Detection Using TOFMS and Triple Quadrupole MS](#) section). This is shown in [Table 2](#) (Figures of merit) for isotopologues with a spacing of $m/z = +1$ and $m/z = +3$ in comparison to the fragment's monoisotopic mass (537.2662), corresponding to 538.2676 and 540.2671, respectively. Evaluating the reliability of analytical results generally comprises also the assessment of trueness. Since trueness is influenced by numerous factors, e.g., sampling and quenching of the metabolism, derivatization, and mass spectrometric analysis, its assessment ideally involves certified reference materials. However, due to the lack of availability, mass spectrometric trueness was assessed by comparing concentration values acquired on both instruments, i.e., GC-TOFMS and GC-MS/MS.

GC-MS/MS Analysis of *Penicillium chrysogenum* Cell Samples. The method was applied for the quantitation of GlcNAc in cell samples of *Penicillium chrysogenum*, more specifically cell extracts, cultivation supernatants, quenching supernatants, and washing supernatants taken at different time points of cell growth. All samples were spiked with the internal standard immediately during the quenching procedure, respectively, after the washing procedure, after filtration or before storage of the biomass. The aliquots of the samples and the ratio of sample to internal standard were adapted according to the sample type ensuring quantification within the method's working range (see the [Experimental Section](#)). By applying this method, GlcNAc concentrations of up to 28 $\mu\text{mol L}^{-1}$ were detectable in samples of the cell extract. Furthermore, GlcNAc was also detectable at significantly lower concentrations in samples of the quenching ($<4.5 \mu\text{mol L}^{-1}$) and washing supernatant ($<0.8 \mu\text{mol L}^{-1}$) as well as in samples of the cultivation supernatant ($<0.7 \mu\text{mol L}^{-1}$). Exemplary chromatograms (GC-EI-MS/MS; 347 \rightarrow 288) of the different sample types are shown in the Supporting Information, [Figure S9](#).

Since GlcNAc is an essential monomer of the fungal cell wall,¹ GlcNAc concentrations depend on the cellular growth. According to this, a high intracellular metabolic pool size is in good accordance to our expectations for growing cells. Since the applied *Penicillium chrysogenum* strain was not over-engineered for GlcNAc production, only low extracellular GlcNAc concentrations were expectable. In case of the cultivation supernatant, the presence of GlcNAc can be reasoned by metabolic segregation by the fungal cells. In contrast, the presence of GlcNAc in the quenching supernatant can be justified by the presence of extracellular GlcNAc in the cultivation supernatant, as well as by a possible cell leakage during the quenching procedure. In the literature, the intracellular and extracellular GlcNAc concentration significantly varies depending for example on the biological host, the applied genetic manipulations, and the biological growth rate. For *Bacillus subtilis* mutants, a short overview was published by Liu et al.³¹ Within this comparison, it was shown that no GlcNAc segregation was detectable for wild-type strains, whereas engineered producer strains with up to 0.25 $\text{mmol g}_{\text{Biomass}}^{-1} \text{h}^{-1}$ are available.³¹

Within our study, apart from *N*-acetylglucosamine, also *N*-acetylgalactosamine was found to be present in extracts of *Penicillium chrysogenum* at concentrations of at least a factor of 10 below GlcNAc concentrations. No ManNAc could be detected. Results obtained for the GlcNAc quantitation in *Penicillium chrysogenum* samples by GC-MS/MS and GC-TOFMS showed good agreement with an average deviation of $2.8 \pm 5.5\%$ ($n = 6$) and a maximum deviation of 12% for samples covering a concentration range from 0.5 to 23 $\mu\text{mol L}^{-1}$.

CONCLUSIONS

A robust and highly selective GC based separation method with mass spectrometric detection for GlcNAc was validated and successfully employed for the analysis of biotechnologically relevant *Penicillium chrysogenum* samples. GlcNAc was detectable in all biological sample types. The presence of GlcNAc in the cultivation supernatant underlines the relevance of a separate sampling/preparation procedure for quenching supernatant, washing supernatant, cultivation supernatant, and cell-extract in combination with a robust quantification method for accurate intracellular balancing of GlcNAc in biological samples. In contrast to matrices like urine or blood plasma, the matrix of biotechnological samples can change vastly in the course of a batch or fed-batch experiment. This highly concentrated matrix clearly leads to a rapid degradation of the performance of the GC-MS system, more specifically S/N ratio and sensitivity. This heavy matrix, together with the strong matrix dependence of the derivatization efficiency, renders internal standardization with stable isotope labeling indispensable.

Nevertheless, the present method proved to be robust, since even after more than 50 injections, concentrations of less than 30 nmol L^{-1} were still possible to be quantified. GC-MS instruments with automated liner exchange and ion source cleaning systems could restore the performance of the system within sequences.

A comparison of MS/MS and TOFMS shows comparable validation results with the exception of the linear range, which is more limited for TOFMS. However, TOFMS shows the advantage of changing data evaluation strategies retrospectively, such as the use of lower abundant isotopologues for

peak integration in case of detector saturation. By this means, the full potential of TOFMS for accurate quantitation can be exploited.

■ ASSOCIATED CONTENT

SI Supporting Information

The Supporting Information is available free of charge at <https://pubs.acs.org/doi/10.1021/acs.analchem.9b04582>.

Figures of results of optimization of inlet temperature, ethoximation parameters, and silylation parameters, chemical structures, EI mass spectra, separation of methoximated and trimethylsilylated *N*-acetylhexosamines using a metabolomics standard column, MS/MS transitions relative sensitivity, GC–TOFMS calibration graphs, GC–MS/MS calibration graphs, and GC–MS/MS chromatograms and tables of exact masses, chemical formulae, and chemical structures (PDF)

■ AUTHOR INFORMATION

Corresponding Author

Christina Troyer – Institute of Analytical Chemistry, Department of Chemistry, University of Natural Resources and Life Sciences, 1190 Vienna, Austria; Phone: +43-1-47654-77192; Email: christina.troyer@boku.ac; Fax: +43-1-47654-77059

Authors

Teresa Mairinger – Institute of Analytical Chemistry, Department of Chemistry, University of Natural Resources and Life Sciences, 1190 Vienna, Austria; orcid.org/0000-0001-7809-1529

Michael Weiner – Novartis Technical Operations Anti-Infectives, MS&T Laboratories, 6250 Kundl, Austria

Stephan Hann – Institute of Analytical Chemistry, Department of Chemistry, University of Natural Resources and Life Sciences, 1190 Vienna, Austria; orcid.org/0000-0001-5045-7293

Complete contact information is available at: <https://pubs.acs.org/doi/10.1021/acs.analchem.9b04582>

Notes

The authors declare no competing financial interest.

■ ACKNOWLEDGMENTS

EQ VIBT GmbH is acknowledged for providing mass spectrometry instrumentation. We thank Philipp Tondl for his help with data evaluation and interpretation. The authors thank the reviewers for their critical input, thereby improving the quality of the paper.

■ REFERENCES

- (1) Konopka, J. B. *Scientifica* **2012**, 2012, 489208.
- (2) Vega, K.; Kalkum, M. *Int. J. Microbiol.* **2012**, 2012, 1–10.
- (3) Edstrom, R. D.; Heath, E. C. *J. Biol. Chem.* **1967**, 242 (16), 3581–3588.
- (4) Sialic Acids. In *Essentials of Glycobiology*; Varki, A., Cummings, R. D., Esko, J. D., Freeze, H. H., Stanley, P., Bertozzi, C. R., Hart, G. W., Etzler, M. E., Eds.; Cold Spring Harbor Laboratory Press: Cold Spring Harbor (NY), 2009.
- (5) Leyn, S. A.; Gao, F.; Yang, C.; Rodionov, D. A. *J. Biol. Chem.* **2012**, 287 (33), 28047–28056.
- (6) Carraway, K. K.; Hull, S. R. *Glycobiology* **1991**, 1, 131–138.
- (7) VandenBoer, T. C.; Di Lorenzo, R. A.; Hems, R. F.; Dawe, K. E. R.; Ziegler, S. E.; Young, C. J. *J. Chromatogr. A* **2020**, 460843.

- (8) Dippold, M. A.; Boesel, S.; Gunina, A.; Kuzyakov, Y.; Glaser, B. *Rapid Commun. Mass Spectrom.* **2014**, 28 (6), 569–576.
- (9) Indorf, C.; Bodé, S.; Boeckx, P.; Dyckmans, J.; Meyer, A.; Fischer, K.; Joergensen, R. G. *Anal. Lett.* **2013**, 46 (14), 2145–2164.
- (10) Kind, T.; Wohlgemuth, G.; Lee, D. Y.; Lu, Y.; Palazoglu, M.; Shahbaz, S.; Fiehn, O. *Anal. Chem.* **2009**, 81 (24), 10038–10048.
- (11) Ruiz-Matute, A. I.; Hernández-Hernández, O.; Rodríguez-Sánchez, S.; Sanz, M. L.; Martínez-Castro, I. *J. Chromatogr. B: Anal. Technol. Biomed. Life Sci.* **2011**, 879 (17–18), 1226–1240.
- (12) Chuanxiang, W.; Lian, X.; Lijie, L.; Fengli, Q.; Zhiwei, S.; Xianen, Z.; Jinmao, Y. *J. Chromatogr. B: Anal. Technol. Biomed. Life Sci.* **2016**, 1011, 14–23.
- (13) Koek, M. M.; Muilwijk, B.; van der Werf, M. J.; Hankemeier, T. *Anal. Chem.* **2006**, 78 (4), 1272–1281.
- (14) Noctor, G.; Bergot, G.; Mauve, C.; Thominet, D.; Lelarge-Trouverie, C.; Prioul, J.-L. *Metabolomics* **2007**, 3 (2), 161–174.
- (15) *Handbook of Derivatives for Chromatography*, 2nd ed.; Blau, K., Halket, J. M., Eds.; John Wiley and Sons Ltd.: West Sussex, England, 1993.
- (16) Katona, Zs. F.; Sass, P.; Molnár-Perl, I. *J. Chromatogr. A* **1999**, 847 (1), 91–102.
- (17) Becker, M.; Liebner, F.; Rosenau, T.; Potthast, A. *Talanta* **2013**, 115, 642–651.
- (18) Kärkkäinen, J.; Vihko, R. *Carbohydr. Res.* **1969**, 10 (1), 113–120.
- (19) Gullberg, J.; Jonsson, P.; Nordström, A.; Sjöström, M.; Moritz, T. *Anal. Biochem.* **2004**, 331 (2), 283–295.
- (20) Neubauer, S.; Haberhauer-Troyer, C.; Klavins, K.; Russmayer, H.; Steiger, M. G.; Gasser, B.; Sauer, M.; Mattanovich, D.; Hann, S.; Koellensperger, G. *J. Sep. Sci.* **2012**, 35 (22), 3091–3105.
- (21) Meinert, S. *Optimization of a Fast Sampling Set up and Two Cultivation Systems for 13C Metabolic Flux Analysis with Penicillium Chrysogenum*; University of Innsbruck, 2012.
- (22) Meinert, S.; Rapp, S.; Schmitz, K.; Noack, S.; Kornfeld, G.; Hardiman, T. *Anal. Biochem.* **2013**, 438 (1), 47–52.
- (23) Vielhauer, O.; Zakhartsev, M.; Horn, T.; Takors, R.; Reuss, M. *J. Chromatogr. B: Anal. Technol. Biomed. Life Sci.* **2011**, 879 (32), 3859–3870.
- (24) Chu, D. B.; Troyer, C.; Mairinger, T.; Ortmayr, K.; Neubauer, S.; Koellensperger, G.; Hann, S. *Anal. Bioanal. Chem.* **2015**, 407 (10), 2865–2875.
- (25) Koek, M. M.; Bakels, F.; Engel, W.; van den Maagdenberg, A.; Ferrari, M. D.; Coulier, L.; Hankemeier, T. *Anal. Chem.* **2010**, 82 (1), 156–162.
- (26) Kanani, H. H.; Klapa, M. I. *Metab. Eng.* **2007**, 9 (1), 39–51.
- (27) Zweckmair, T.; Schiehser, S.; Rosenau, T.; Potthast, A. *Carbohydr. Res.* **2017**, 446–447, 7–12.
- (28) Fontaine, T.; Delangle, A.; Simenel, C.; Coddeville, B.; van Vliet, S. J.; van Kooyk, Y.; Bozza, S.; Moretti, S.; Schwarz, F.; Trichot, C.; et al. *PLoS Pathog.* **2011**, 7 (11), No. e1002372.
- (29) Mashego, M. R.; Wu, L.; Van Dam, J. C.; Ras, C.; Vinke, J. L.; Van Winden, W. A.; Van Gulik, W. M.; Heijnen, J. J. *Biotechnol. Bioeng.* **2004**, 85 (6), 620–628.
- (30) Magnusson, B.; Örnemark, U. *Eurachem Guide: The Fitness for Purpose of Analytical Methods – A Laboratory Guide to Method Validation and Related Topics*, 2nd ed.; 2014.
- (31) Liu, Y.; Link, H.; Liu, L.; Du, G.; Chen, J.; Sauer, U. *Nat. Commun.* **2016**, 7 (1), 11933.